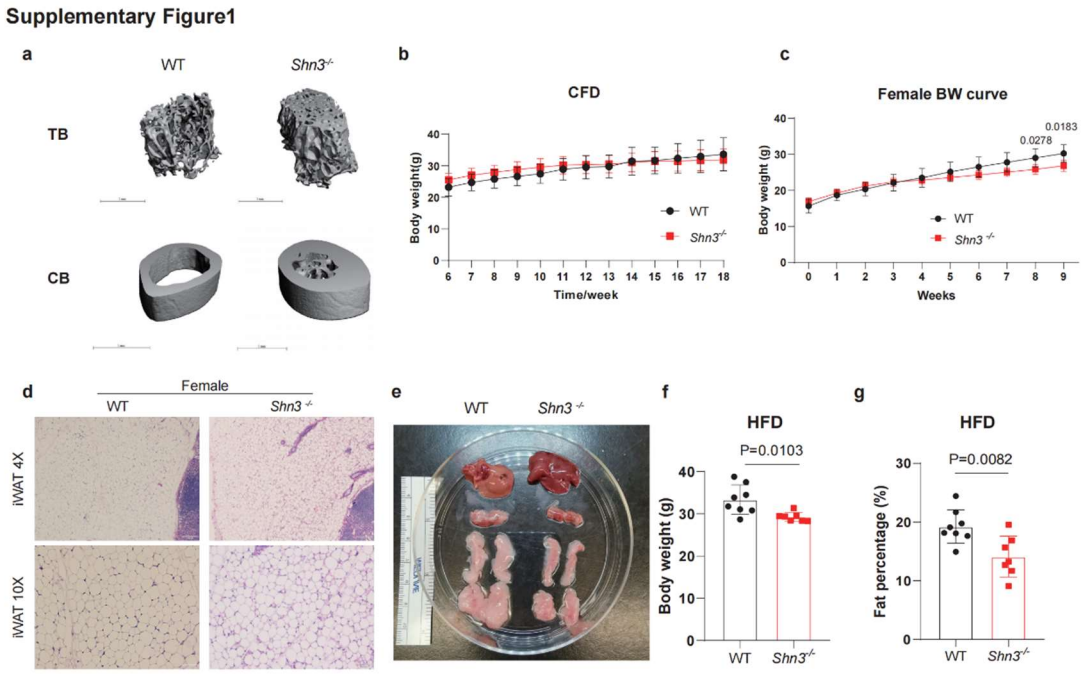
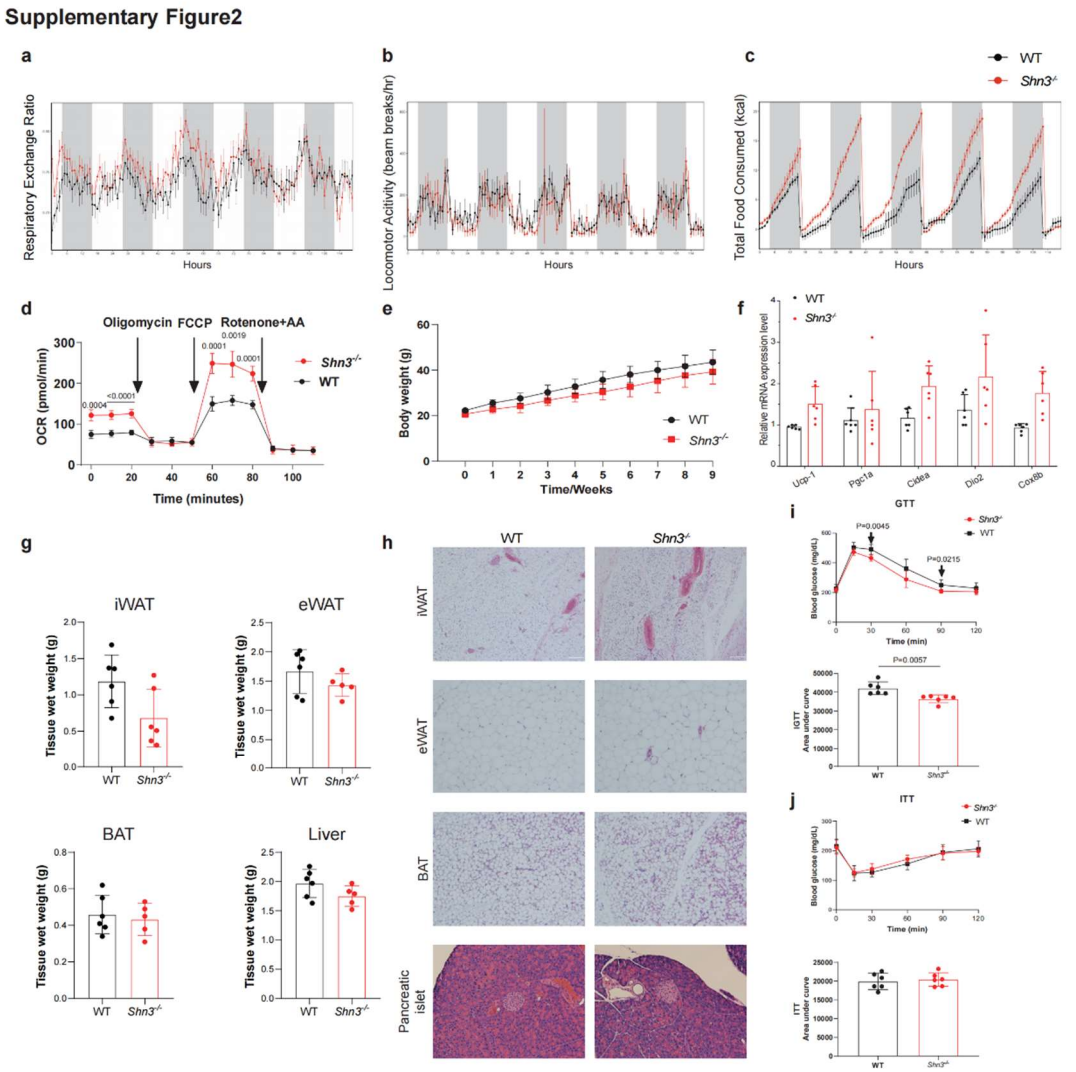
Supplementary materials



Supplementary Figure 1 *Shn3*$^{-/-}$ mice are resistant to DIO with dysfunctional glucose homeostasis

(a) μCT representative images of trabecular (TB) and cortical bone (CB) of WT and *Shn3*$^{-/-}$ mice. (b) Body weight curve of control-fat-diet fed WT and *Shn3*$^{-/-}$ mice (n=5). (c) Body weight curve of HFD-fed WT and *Shn3*$^{-/-}$ female mice (n=6). (d) Representative histological results of iWAT of HFD-fed WT and *Shn3*$^{-/-}$ female mice from 3 individual slides. (e) General view of liver, BAT, iWAT and eWAT of WT and *Shn3*$^{-/-}$ Balb/c background mice after 12-week HFD feeding. (f) End point body weight of 12-week HFD-fed WT and *Shn3*$^{-/-}$ Balb/c mice. (g) Body composition of WT and *Shn3*$^{-/-}$ Balb/c background mice through echo-MRI. Results were presented as mean ± s.d., analyzed by unpaired, two-tailed Student's t test (f, g) or two-way ANOVA with Bonferroni's multiple comparisons test (b, c).



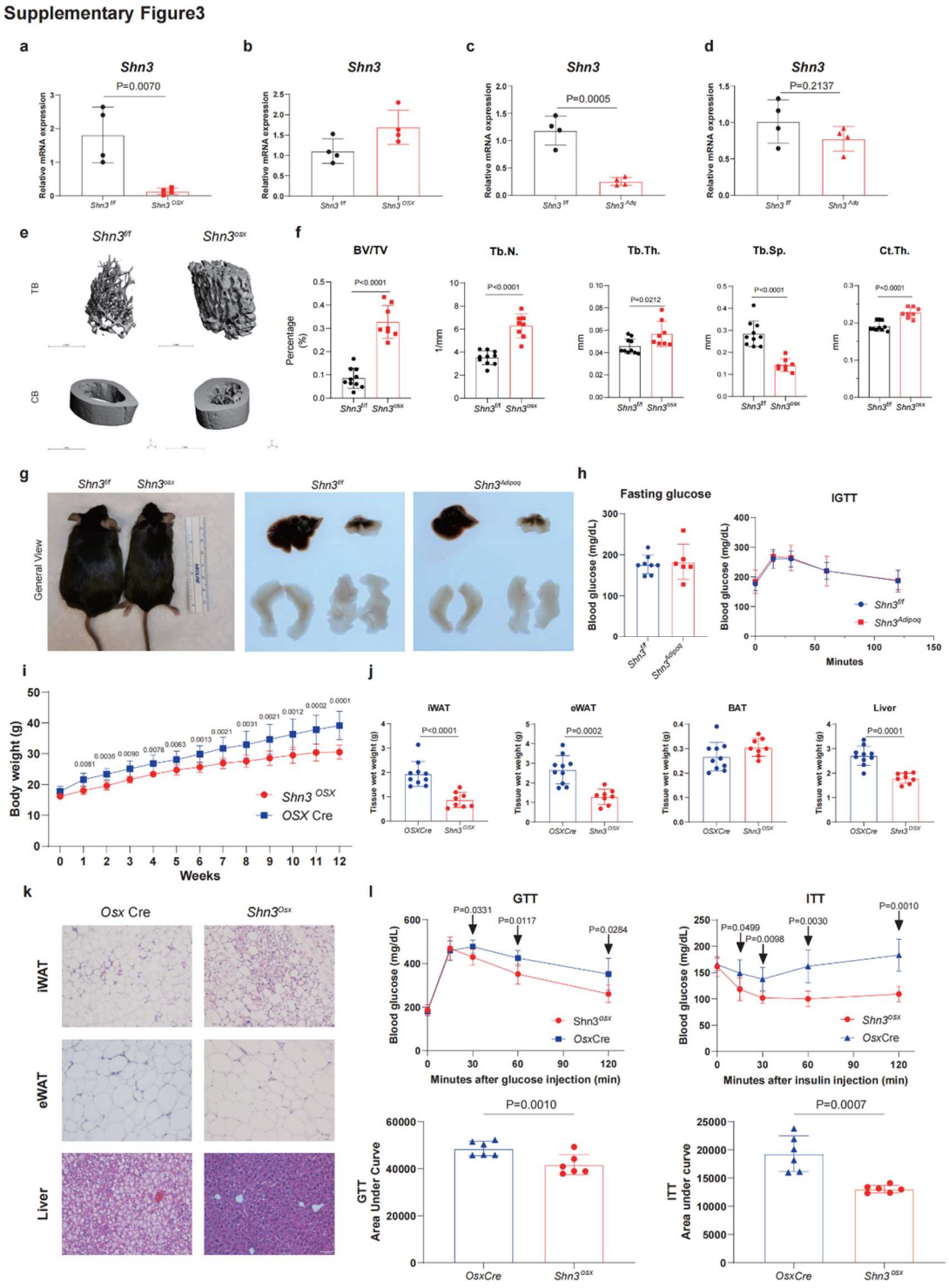
Supplementary Figure 2 Increased energy expenditure and WAT browning in *Shn3*$^{-/-}$ mice

(a) Respiratory exchange ratio, (b) locomotor activity and (c) total food consumption of HFD-fed WT and *Shn3*$^{-/-}$ mice housed under room temperature (n=7 for WT group, n=6 for *Shn3*$^{-/-}$ group). (d) Mitochondrial stress test displaying the oxygen consumption rate (OCR) of primary adipocytes harvested from HFD-fed WT and *Shn3*$^{-/-}$ mice (n=5 for each group, *P* values directly labeled above the time points).

For thermoneutral housing experiments, data and samples were collected from C57BL6/J background littermate male WT (n=6) and *Shn3*$^{-/-}$ mice (n=6) after HFD feeding under thermoneutral condition (housing temperature 30^{o}C) for 10 weeks. (e) Body weight curve obtained during 9 weeks HFD feeding started from 6-week-old age. (f) Expression level of thermogenic genes in iWAT from WT and *Shn3*$^{-/-}$ mice measured by qPCR. (g) Tissue wet weight of liver, BAT, iWAT and eWAT of WT and *Shn3*$^{-/-}$ mice. (h) Representative

histological sections of iWAT, eWAT, BAT and pancreatic islet from 3 individual slides. Scale bar=200um. (i) IGTT and (j) ITT results of TN-HFD-fed WT and *Shn3*$^{-/-}$ mice (*P* values directly labeled above the time points). Results were collected from 6 repeated experiments.

Results were presented as mean ± s.d., analyzed by unpaired, two-tailed Student's t test (f, g and lower of i-j) or two-way ANOVA with Bonferroni's multiple comparisons test (a-e and upper of i-j). ***P*<0.005, ****P*<0.0005.

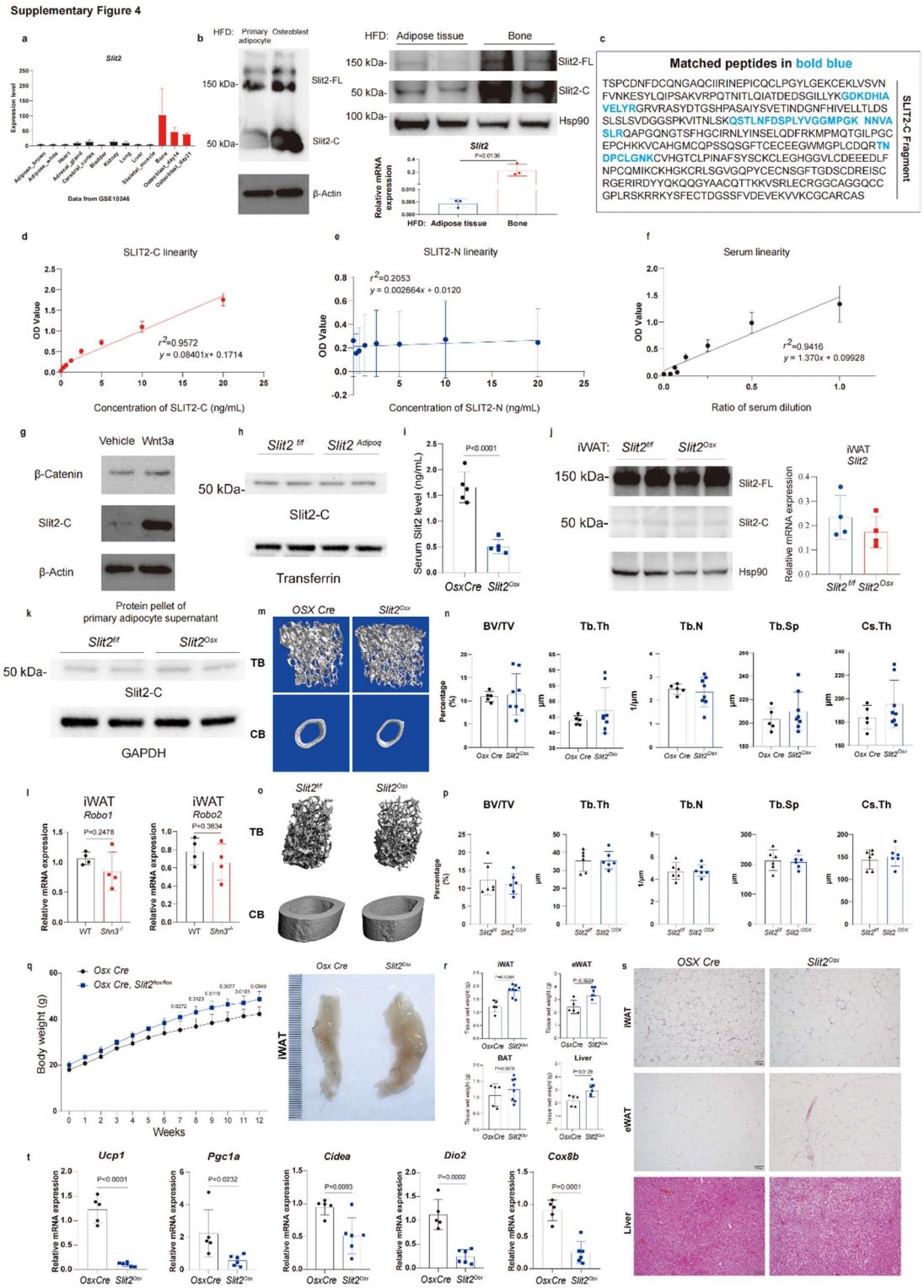


Supplementary Figure 3 Deletion of *Shn3* in osteoblasts but not adipocytes recapitulates resistance to DIO

qPCR quantification of *Shn3* expression level in (a) bone and (b) iWAT of *Shn3*$^{f/f}$ and *Shn3*^{Osx} mice. qPCR quantification of *Shn3* expression level in (c) iWAT and (d) bone of *Shn3*$^{f/f}$ and *Shn3*^{Adipoq} mice.

(e) μCT representative images of trabecular (TB) and cortical bone (CB) of *Shn3*^{Osx} and *Shn3*$^{f/f}$ mice. (f) μCT analysis of bone volume/total volume

(BV/TV), trabecular number (Tb.N.), trabecular thickness (Tb.Th.), trabecular spacing (Tb.Sp.) and cortical thickness (Ct.Th.) from *Shn3*^{Osx} and *Shn3*$^{f/f}$ mice femurs. (g) Gross images of HFD-fed *Shn3*^{Osx} and *Shn3*$^{f/f}$ mice (left) and liver (upper left of middle and right), BAT (upper right of middle and right), iWAT (lower left of middle and right) and eWAT (lower right of middle and right) from *Shn3*^{Adipoq} and *Shn3*$^{f/f}$ mice after 12-week HFD exposure. (h) Fasting glucose levels and IGTT results of HFD-fed *Shn3*^{Adipoq} and *Shn3*$^{f/f}$ mice. (i) Body weight curve of male *Shn3*^{OSX} and *Osx* Cre mice mice after HFD for 12 weeks (n=10 for each group, *P* values directly labeled above the time points). (j) Tissue wet weight of iWAT, eWAT, BAT and liver from HFD-fed *Shn3*^{OSX} and *Osx* Cre mice. (k) Representative histological sections of iWAT, eWAT and liver from 3 individual slides of *Shn3*^{OSX} and *Osx* Cre mice. Scale bar=200um. (l) Results of intraperitoneal glucose tolerance and insulin tolerance tests (*P* values directly labeled above the time points) and the area under the curve for *Shn3*^{Osx} and *Osx* Cre mice is shown (n=6 for each group). The mouse cohort in Supplementary Fig. 3i-j is distinct from that displayed in Figure. 3. Results were presented as mean ± s.d., analyzed by unpaired, two-tailed Student's t test (a-f, left of h and lower of l) or two-way ANOVA with Bonferroni's multiple comparisons test (right of h, l and upper of l).

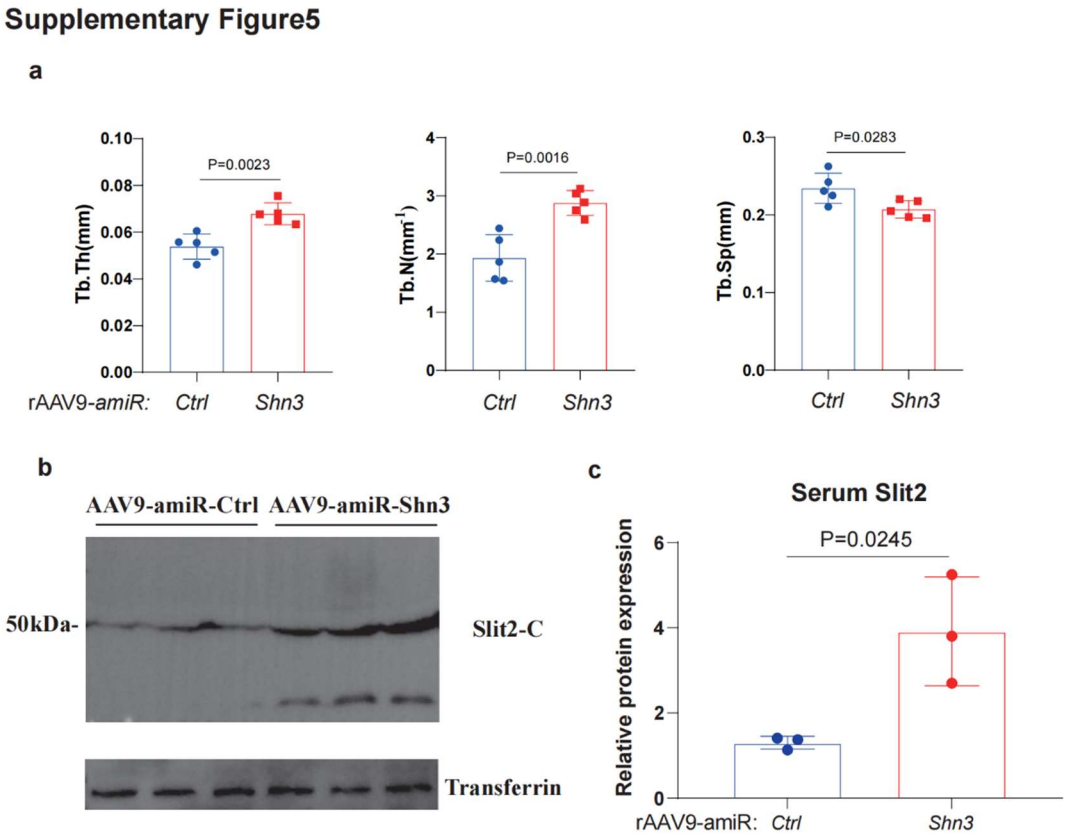


130

131 **Supplementary Figure 4 SLIT2 is an osteokine secreted by osteoblasts**
132 **that protects mice from DIO**

133 (a) A tissue gene expression array displaying *Slit2* expression. GSE10246
134 was used as a data source, and data is presented as mean ± s.d.. (b)
135 Immunoblots of Slit2 in differentiated osteoblasts, primary adipocytes (left),
136 adipose tissue and bone (upper right) along with qPCR results displaying *Slit2*

expression level in adipose tissue and bone (lower right, n=3 for each group) harvested from HFD-fed murine models. (c) Matched peptides of SLIT2 and related sequence of amino acids detected in the precipitate of osteoblast supernatant. Validation of ELISA kit linearity through serial dilution of recombinant (d)SLIT2-C, (e)SLIT2-N fragment and (f)serially diluted murine samples (n=3 for each experiment). (g) Immunoblots of β-catenin, SLIT2-C and β-Actin of vehicle (Vehicle) and Wnt3a (Wnt3a, 200ng/mL) treated osteoblasts. (h) Serum SLIT2-C level in *Slit2*^{Adipoq} and *Slit2*$^{f/f}$ mice. (i) Serum SLIT2-C level assessed by ELISA in HFD-fed *Slit2*^{Osx} and *Osx* Cre mice (n=5 for each group). (j) Immunoblot (left) and qPCR (right) quantification of Slit2 level in iWAT of HFD-fed *Slit2*^{Osx} and *Slit2*$^{f/f}$ mice. (k) Western Blot result of SLIT2-C in supernatant of primary inguinal cells isolated from HFD-fed *Slit2*^{Osx} and *Slit2*$^{f/f}$ mice. (l) Expression level of *Robo1* and *Robo2* in iWAT from WT and *Shn3*$^{-/-}$ mice quantified by qPCR (n=4 for each group). (m) μCT reconstruction of trabecular (TB) and cortical bone (CB) of HFD-fed *Slit2*^{Osx} and *Osx* Cre mice. (n) Bone μCT analysis of HFD-fed *Slit2*^{Osx} and *Osx* Cre mice (n=5 for *Osx* Cre group and n=8 for *Slit2*^{Osx} group). (o) μCT reconstruction of trabecular (TB) and cortical bone (CB) of HFD-fed *Slit2*^{Osx} and *Slit2*$^{f/f}$ mice. (p) Bone μCT analysis of HFD-fed *Slit2*^{Osx} and *Slit2*$^{f/f}$ mice (n=6 for each group). (q) Body weight curve (left) and gross view of iWAT (right) of *Slit2*^{Osx} and *Osx* Cre mice obtained during 12 weeks HFD feeding started from 6-week-old age (n=5 for *Osx* Cre group and n=8 for *Slit2*^{Osx} group, *P* values directly labeled above the time points). (r) Tissue wet weight of iWAT, eWAT, BAT and liver from HFD-fed *Slit2*^{Osx} and *Osx* Cre mice. (s) Representative histological sections of iWAT, eWAT and liver (results from 3 individual experiments). (t) Thermogenic gene expression level in iWAT of HFD-fed *Slit2*^{Osx} and *Osx* Cre mice (n=5 for each group). The mouse cohort in Supplementary Fig. 4n-q is distinct from that displayed in Fig. 5. Results were presented as mean ± s.d., analyzed by unpaired, two-tailed Student's t test (b, i, j, l, n, p, r and t), linear regression (d-f) or two-way ANOVA with Bonferroni's multiple comparisons test (q). **P*<0.05, ***P*<0.005, ****P*<0.0005.



Supplementary Figure 5 AAV-mediated skeletal SHN3 depletion reduced development of DIO and metabolic syndrome

(a) Analysis of μCT reconstruction results showing trabecular number (Tb. N), trabecular thickness (Tb. Th) and trabecular separation (Tb. Sp) of rAAV9-amiR-*Shn3* and rAAV9-amiR-*Ctrl* injected mice (n=5 for each group). (b) Immunoblots and (c) quantification of Slit2-C level in sera collected from HFD-fed, rAAV9-amiR-*Shn3* and rAAV9-amiR-*Ctrl* injected mice (n=3 for each group). Results were presented as mean ± s.d., analyzed by unpaired, two-tailed Student's t test (a and c).

Supplementary Table 1 Primer list for qPCR analysis

Gene symbols	Forward sequence	Reverse sequence
Gapdh	CATCACTGCCACCCAGAAGACTG	ATGCCAGTGAGCTTCCCGTTCAG
Ucp1	GCTTTGCCTCACTCAGGATTGG	CCAATGAACACTGCCACACCTC
Pgc1a	TATGGAGTGACATAGAGTGTGCT	CCACTTCAATCCACCCAGAAAG
Cidea	GGTGGACACAGAGGAGTTCTTTC	CGAAGGTGACTCTGGCTATTCC
Dio2	GGTGGTCAACTTTGGTTCAGCC	AAGTCAGCCACCGAGGAGAACT
Cox8b	GCGAAGTTCACAGTGGTTCC	GGAACCATGAAGCCAACGAC
Slit2	ACCGTCTGAGATGTATCCCTCC	GCTGACAAGTCATTGAAGGCACC
Hivep3	CTGGTTCCATCCAACTCCCGAA	CCTCTCTTGGAAGTGGGAGTAC
Acads	GACTGGCGACGGTTACACA	GGCAAAGTCACGGCATGTC
Acadm	AGGATGACGGAGCAGCCAATGA	GCCGTTGATAACATACTCGTCAC
Acadl	GGCGATTTCTGCCTGTGAGTTC	GCTGTCCACAAAAGCTCTGGTG
Acadvl	GAGAAGGTGGAGGACGACACTT	CACAATCTCTGCCAAGCGAGCA
Cpt1a	GGCATAAACGCAGAGCATTCCTG	CAGTGTCCATCCTCTGAGTAGC
Hadha	GTTTGAGGACCTCGGTGTAAAGC	GAGAGCAGATGTGTTGCTGGCA
CD36	GGACATTGAGATTCTTTTCCTCTG	GCAAAGGCATTGGCTGGAAGAAC
Robo1	GGCAGCCTGTTGGATTATCCTC	GTTGGCGTGAAGGTAAAGGACG
Robo2	CCACCATCCAAACCTCAGGTCA	TCTGCCAGCTATTGCTCACCGA